Docosahexaenoic acid and oleic acid induce altered DNA methylation of individual CpG loci in Jurkat T cells

J. Eduardo Pérez-Mojica[1], Karen A. Lillycrop[2], Cyrus Cooper[3], Philip C. Calder[1], Graham C. Burdge[1]

[1]*School of Human Development and Health, Faculty of Medicine, University of Southampton, Southampton, UK.*
[2]*Centre for Biological Science, Faculty of Natural and Environmental Sciences, University of Southampton, Southampton, UK.*
[3]*MRC Lifecourse Epidemiology Unit, University of Southampton, Southampton General Hospital, Southampton, UK*

Correspondence to: Professor G.C. Burdge, School of Human Development and Health, Institute of Developmental Sciences Building (MP887), Faculty of Medicine, University of Southampton, Southampton General Hospital, Tremona Road, Southampton, SO16 6YD, UK. g.c.burdge@soton.ac.uk. Telephone +44(0)2381205259

Financial support
The study was funded by The Medical Research Council (UK) and The National Council for Science and Technology (CONACYT) (Mexico).

Key words Docosahexaenoic acid, Oleic acid, DNA methylome, PPARα, Response element, Jurkat cells.

Abbreviations

DHA, docosahexaenoic acid; pTRE, putative transcription factor response element; PPARRE peroxisomal proliferator activated receptor response element; PUFA, polyunsaturated fatty acid

Abstract

Docosahexaenoic acid (DHA, 22:6n-3) and oleic acid (18:1n-9) can alter the DNA methylation of individual CpG loci *in vivo* and *in vitro,* although the targeting mechanism is unknown. We tested the hypothesis that the targeting of altered methylation is associated with putative transcription factor response elements (pTREs) proximal to modified loci. Jurkat cells were treated with 22:6n-3 or 18:1n-9 (both 15 μM) for eight days and DNA methylation measured using the MethylationEPIC 850K array. 1596 CpG loci were altered significantly (508 hypermethylated) by 22:6n-3 and 563 CpG loci (294 hypermethylated) by 18:1n-9. 78 loci were modified by both fatty acids. Induced differential methylation was not modified by the PPARα antagonist GW6471. DNA sequences proximal to differentially methylated CpG loci were enriched in zinc-finger pTREs. These findings suggest that zinc-finger-containing transcription factors may be involved in targeting altered DNA methylation modifying processes induced by fatty acids to individual CpG loci.

1. Introduction

Fatty acids can modify cell function by influencing cell membrane fluidity and, consequently the activity of integral proteins, by changing the nature of lipid second messengers and by altering the expression of the transcriptome, for example via the induction of peroxisome proliferator-activated receptor (PPAR) activity [1]. In addition, there is increasing evidence that fatty acids can alter cell function via inducing changes in epigenetic processes [2]. For example, feeding pre-pregnant and pregnant mice diets with different 18:2n-6 : 18:3n-3 ratios has been shown to induce in the offspring modest changes in the mean DNA methylation of the *Fads2* promoter [3]. The offspring of pregnant rats fed diets with different saturated or polyunsaturated fatty acid (PUFA) contents induced in the offspring hypermethylation, up to a 20% difference in DNA methylation, of specific CpG loci in the *Fads2* promoter and decreased mRNA expression of the gene [4]. Dietary supplementation of humans with either omega-3 PUFA, ethyl esters of 20:5n-3, 22:5n-5 and 22:6n-3, or olive oil induced CpG locus-specific changes in the DNA methylation of *FADS2* and *ELOVL5*, but not *FADS1* or *ELOVL2*, which differed in locus, direction and magnitude between dietary supplements and between men and women, which was reproducible in two cohorts [5]. Dietary supplementation of pregnant women with 22:6n-3 induced modest (< 5%) changes in the DNA methylome of their infants [6]. Moreover, incubation of U937 leukaemic cells with 20:5n-3 induced demethylation of a single CpG locus in the CC/AAT/enhancer binding protein-δ promoter and increased expression of the gene, while there was no effect of incubation with 18:1n-9 [7, 8]. Treatment of THP-1 monocytes with either 20:4n-6 or 18:1n-9 induced fatty acid concentration-related changes in global DNA methylation [9]. Overall, fatty acids can alter the epigenetic regulation of specific genes in a manner that appears to depend upon the type of fatty acid used. However, the mechanisms by which fatty acids induce locus-specific changes in DNA methylation are not known, although binding of PPARα to its response element has been suggested to be involved in the targeting of the fatty acid to individual CpGs [9].

To address this mechanism, we determined the effect of incubating Jurkat T cells with either 22:6n-3 or 18:1n-9 on the DNA methylome using the MethylationEPIC 850K array. We then investigated whether PPARα was involved in the induction of altered DNA methylation of individual CpG loci, and if differentially methylated loci were enriched for specific transcription factor binding sites.

2. Materials and methods

2.1 Cell culture

Jurkat cells were maintained in RPMI-1640 medium (Sigma-Aldrich, Dorset, UK) supplemented

with 9% (v/v) fetal bovine serum (Life Technologies, Renfrewshire, UK), 2 mM L-glutamine, 100 U/mL penicillin and 100 µg/mL streptomycin (Sigma-Aldrich, Dorset, UK) and incubated at 37 ºC in an atmosphere containing 5% (v/v) CO_2. Cells were treated with either 22:6n-3 or 18:1n-9 (both 15 µM) (Sigma-Aldrich, Dorset, UK) or ethanol carrier (final concentration < 0.05% (v/v)) (n = 12 replicate cultures per treatment) for up to 8 days. The concentrations of 18:1n-9 and 22:6n-3 were comparable to those reported in human blood lipids [10]. In some experiments, Jurkat cells were treated with the PPARα antagonist GW6471 (2 µM) (both Bio-Techne, Oxfordshire, UK) plus 22:6n-3 (15 µM) (n = 8 replicate cultures per treatment). In all experiments, culture medium was replaced every 72 hours. Cell viability was measured by trypan blue exclusion (Sigma-Aldrich, Dorset, UK). At the end of the incubation period, cells were harvested by centrifugation, washed three times with phosphate-buffered saline (PBS) (Sigma-Aldrich, Dorset, UK) and stored at -80 ºC.

2.2 Measurement of fatty acid composition by gas chromatography

The fatty acid composition of the cells was determined essentially as described previously [11]. Cells ($8x10^6$) were washed three times with PBS and resuspended in 0.9% (w/v) NaCl (0.8 ml). Chloroform/ methanol 2:1 (v/v) (5 ml) (Fisher-Scientific, Leicestershire, UK) containing butylated hydroxytoluene (50 mg/l) and 1M NaCl (1 ml) were added, the samples vortexed, and the organic phase then collected and dried under N_2 [12]. The dried extract was dissolved in toluene and fatty acid methyl esters (FAME) were synthesised by incubation with methanol containing 2% (v/v) sulphuric acid at 50 ºC for 2 hours [11]. FAME were extracted with hexane and resolved on a BPX-70 fused silica capillary column (32 m × 0·25 mm × 25 µm; SGE Analytical Science) using an Agilent 6890 gas chromatograph equipped with flame ionisation detection (Agilent Technologies Ltd) [10]. Peaks were identified by comparison of retention times with authentic standards (Supelco® 37 Component FAME Mix, Sigma).

2.3 Analysis of DNA methylation

Genomic DNA was extracted using QIAamp DNA Blood Mini Kit (Qiagen, Manchester, UK) according to the manufacturer's instructions. DNA concentration and purity were measured using a NanoDrop ND-1000 full-spectrum (λ = 220-750 nm) spectrophotometer (Thermo Scientific, UK) where λ = 260/280 and λ = 260/230 ratios were all 1.8 (± 0.1) and 2.2 (± 0.2), respectively. DNA samples with the highest concentration (n = 4 replicate cultures per treatment) were then analysed using the Infinium MethylationEPIC 850K array (Illumina, San Diego, CA) that measured the DNA methylation status of 864,935 CpG sites by single-base extension [13]. Array

hybridisation was carried out by the Centre for Molecular Medicine and Therapeutics, BC Children's Research Hospital Institute, University of British Columbia, Vancouver, Canada. Raw data were analysed with the R package minfi version 1.18.6 [14] with MethylationEPIC annotation ilm10b2.hg19_0.3.0 and the R version 3.3.0 of the IRIDIS 4 High-Performance Computing Facility at the University of Southampton (Southampton, UK). Standard quality controls and normalisation procedures were followed for the data pre-processing [15]. 1,047 (22:6n-3) and 1,038 (18:1n-9) poor quality probes were excluded from the analysis according to a mean detection p-value > 0.05 of the absolute signal (methylated + unmethylated) compared to background [15]. 28,931 (22:6n-3) and 28,928 (18:1n-9) SNP disrupting probes were also excluded from the analysis [16]. Normalisation was carried out using functional normalisation (Funnorm) which clustered the β-densities of all samples as expected (Supplemental Figure 1) [17]. Complete removal of batch effects was achieved using the ComBat function (Supplemental Figure 2) [18] included in the sva R package. Samples were categorically clustered and CpG loci with P-value < 0.05, q-value < 0.05 (Benjamini and Hochberg False Discovery Rate for multiple testing correction [19]) and a β-value > 0.05 were considered to be differentially methylated. An overview of analysis workflow is shown in Supplemental Figure 3.

2.4 Pyrosequencing

Pyrosequencing was performed as described previously [20]. Briefly, genomic DNA (1µg), EpiTect Control DNA unmethylated (Qiagen, West Sussex, UK) and CpGenome^{TM} Universal Methylated DNA (Millipore, Hertfordshire, UK) were bisulphite converted using the EZ DNA Methylation-Gold™ Kit (Cambridge Bioscience, Cambridge, UK) according to the manufacturer's instructions. PCR was then performed using bespoke primers (Table 1) (Eurofins Genomics, Ebersberg, Germany) in a final reaction volume of 25 µl. 45 PCR cycles were performed, each cycle comprising of denaturation at 95 ºC for 15 s, annealing at probe-specific temperature (Table 1) for 30 s and extension at 72 ºC for 15 s using KAPA2G Robust HotStart ReadyMix Kit (Kapa Biosystems, Massachusetts, USA). PCR amplification was assessed using agarose gel electrophoresis. Pyrosequencing was carried out as described [21]. Briefly, PCR products were immobilised on Streptavidin Sepharose® High-Performance beads (34 µm, GE Healthcare Life Sciences, Buckinghamshire, UK), washed, denatured and eluted into annealing buffer that contained the sequencing primers (Table 1). DNA methylation was measured using the SQA kit on a PSQ 96MA Pyrosequencer (Biotage AB, Kungsgatan, Sweden). Percent DNA methylation was calculated using Pyro Q CpG software (Biotage).

2.5 Pathway analyses

Canonical pathways enriched for differentially methylated genes were identified using Ingenuity® Pathway Analysis (IPA®) software (QIAGEN Bioinformatics). Analysis was carried out using the built version: 400896M, content version: 28820110 (release date: 2018-09-24). All CpG loci with significantly altered DNA methylation within any genic region were considered for analysis. Excluding duplicates, 935 or 348 genes in cells treated with 22:6n-3 or 18:1n-9, respectively, were mapped by the IPA® software and included in the analysis. Statistical significance was assumed at $P < 0.05$ from Fisher's exact performed in IPA® using a dataset containing all genes included in the 850K array (background restricted).

2.6 DNA Motif Analysis

All differentially methylated CpG loci in cells treated with 22:6n-3 or 18:1n-9 were tested for the presence of DNA motifs and compared to $1x10^5$ unmodified CpG loci as control. The number for control CpG loci was the maximum number possible to use that was unaltered in the same genomic context. To cover the majority of DNA binding sites in eukaryotes (typically < 30 bp in length) [22] we screened ± 60 bp proximal to each CpG locus. To increase reliability of the results, motif analysis was carried out using two different publicly available tools, namely Multiple EM (Expectation maximisation algorithm) for Motif Elicitation (MEME) and Hypergeometric Optimisation of Motif EnRichment (HOMER) [23, 24]. *De novo* motif discovery was performed in both tools using discriminative analysis with zero or one occurrence per sequence (ZOOPS) scoring. DNA motifs with an expected value (E-value) $\leq 1x10^{-10}$ by MEME or HOMER were then compared using the similarity, tree-building, and alignment of DNA motifs and profiles (STAMP) tool [25, 26]. Only similar motifs (STAMP E-value < 0.05) identified by both tools were individually compared with the core collection of the HOmo sapiens COmprehensive MOdel COllection (HOCOMOCO) v11 using the Tomtom tool in the MEME Suite [27, 28]. DNA motifs with an E-value < 0.05 and q-value < 0.05 were considered to be similar to putative response elements. An overview of the motif analysis workflow is shown in Supplemental Figure 4.

2.7 Statistics

Statistical analyses were carried out using IBM SPSS® version 22.0.0.0, 64-bit edition. Statistical significance was assumed at $P < 0.05$. Controls versus treatment means were compared using either Students t-test or ANOVA as specified in the table or figure legend.

3. Results

3.1 Effect of 22:6n-3 and 18:1n-9 treatment on the fatty acid composition and viability of Jurkat cells

Treatment of Jurkat cells with 22:6n-3 for 8 days increased the proportions of 22:6n-3 (11.9-fold), 16:0 (1.5-fold), 18:0 (1.4-fold), 20:3n-3 (2.1 -fold), 20:5n-3 (3.8 -fold) and 22:5n-3 (2.2 -fold), and decreased the proportions of 16:1n-7 (1.26-fold), 18:1n-9 (1.1-fold) and 18:1n-7 (-1.26-fold) (Figure 1A). Incubation of Jurkat cells with 18:1n-9 for 8 days increased the proportions of 18:1n-9 (2.9-fold), 16:0 (1.2-fold) and 20:1n-9 (4.4-fold), but decreased the proportion of 16:1n-7 (1.3-fold) (Figure 1B). The viability of Jurkat cells treated with 18:1n-9 or 22:6n-3 was > 90% throughout the experiments.

3.2 Effect of fatty acid treatment on DNA methylation in Jurkat Cells

Unsupervised principle component analysis of all CpG loci included in the array did not show complete divergence between treatment groups (Figure 2A). However, restricting the analysis to differentially methylated CpG loci ($P < 0.05$; q-value < 0.05, $\Delta\beta > 0.05$) showed complete clustering of samples according to treatment (Figure 2B).

1596 CpG sites were differentially methylated (P-value < 0.05, q-value < 0.05, β-value > 0.05) in Jurkat cells treated with 22:6n-3 compared to controls, of which 508 (32%) were hypermethylated (Figure 3A). 563 CpG loci were differentially methylated in cells treated with 18:1n-9, of which 294 (52%) were hypermethylated (Figure 3B). 78 CpG loci that were differentially methylated (26 (33%) hypermethylated) in cells treated with 22:6n-3 were also differentially methylated in cells treated with 18:1n-9. The direction of change in methylation of CpG loci that were altered by both 22:6n-3 and 18:1n-9 was the same for both treatments (Figure 3; Supplemental Table 2).

3.3 The genomic distribution of differentially methylated CpG loci in Jurkat cells treated with 22:6n-3 or 18:1n-9

The ratio of CpG altered to CpG measured was calculated in order to adjust the data for any effect of the distribution bias of CpG loci detected by the 850K array in genic regions (defined here as the region -1500 bp to the transcription start site to the 3' UTR, n = 616,132 loci) compared to intergenic regions (n = 248,803 loci). Treatment with 22:6n-3 induced differential DNA methylation of 0.16% CpG loci at genic regions and 0.24% CpG loci at intergenic regions. 18:1n-9 induced differential DNA methylation on 0.06% CpG loci at genic regions and 0.09% CpG loci at intergenic regions. A higher ratio in CpG loci within intergenic regions compared to CpG loci

within genic regions was also observed when altered CpG loci were analysed according to the direction of change in DNA methylation. Incubation with 22:6n-3 induced hypermethylation of 0.05% CpG loci in genic regions and 0.07% in intergenic regions. 22:6n-3 induced hypomethylation of 0.11% loci in genic regions and 0.17% loci in intergenic regions. Incubation with 18:1n-9 induced hypermethylation of 0.03% loci in genic sequences and 0.05% loci in intergenic regions. 18:1n-9 also induced hypomethylation of and 0.03% loci in genic regions and 0.04% loci in intergenic regions.

3.4 *Pathway analysis of differentially methylated genes in Jurkat cells treated with 22:6n-3 or 18:1n-9*

Treatment with 22:6n-3 or 18:1n-9 changed the DNA methylation of 988 or 345 CpG loci, respectively, in genic regions. Genes with altered DNA methylation induced by 22:6n-3 were enriched in genes involved in Synaptic Long-Term Potentiation, Synaptic Long-Term Depression, Protein Kinase A Signalling, and Netrin Signalling canonical pathway (Table 2). Genes with altered DNA methylation induced by 18:1n-9 were associated with Amyotrophic Lateral Sclerosis Signalling, Opioid Signalling Pathway, Aryl Hydrocarbon Receptor Signalling, and Clathrin-mediated Endocytosis Signalling canonical pathways (Table 2).

3.5 Validation of 850K array by pyrosequencing

The methylation status of loci that were shown to be differentially methylated on the 850K array was validated by pyrosequencing. Three CpG loci that had lower DNA methylation (ID cg26292058, cg05475386, and cg27188282) and two CpG loci that had higher DNA methylation (ID cg06989443 and cg22518417) than controls after incubation with 22:6n-3 were used for validation analysis. These loci were within the top twenty most differentially methylated CpG loci and were within a sequence that allowed primer design. All CpG loci analysed by pyrosequencing showed a significant change on DNA methylation in the same direction as the 850K array. The magnitude of DNA methylation change in treatments compared with controls was comparable between both methods (Supplemental Table 1).

3.6 Time course of the induction of altered DNA methylation by 22:6n-3

The level of methylation of the 5 CpG loci used for array validation was measured by pyrosequencing after incubation with 22:6n-3 for 3, 6 and 8 days. There was a significant treatment effect and a significant time*treatment effect on the methylation status of cg26292058 (treatment $P < 0.0001$; time*treatment $P = 0.002$), cg05475386 (treatment $P < 0.0001$; time*treatment P =

0.006), cg6989443 (treatment and time*treatment both P< 0.0001) and cg22518417 (treatment P < 0.0001; time*treatment P = 0.002), and a significant effect of treatment on cg27188282 (P = 0.001). 18:1n-9 did not alter the methylation status of any of the CpG loci measured (Figure 4). Incubation with 22:6n-3 altered the methylation status of cg26292058, cg27188282 and cg22518417 compared to untreated cells by 8 days, but not at earlier time points, while the methylation status of the other CpG loci that were measured differed from untreated cells by 6 days (Figure 4).

3.7 The effect of treatment with a PPARα antagonist on induction of altered DNA methylation by 22:6n-3

The PPARα antagonist GW6471 has been shown to inhibit induction of altered DNA methylation by 20:4n-6 in THP-1 monocytes [9]. Therefore, we investigated whether GW6471 altered the effect of 22:6n-3 on the DNA methylation status of the 5 CpG loci used for array validation. There was a significant effect on the methylation status of all 5 candidate loci (all P < 0.01) in cells treated with 22:6n-3 only or 22:6n-3 plus GW6471 (Figure 5). However, there was no significant difference in the change in DNA methylation induced by 22:6n-3 and that induced by 22:6n-3 plus GW6471 at these 5 CpG loci.

3.8 Identification of DNA motifs in sequences containing differentially methylated CpGs in cells treated with 22:6n-3 or 18:1n-9

DNA motif analysis was carried out using data obtained from Jurkat cells treated with 22:6n-6 or 18:1n-9. Twenty-seven pTREs were significantly aligned (P < 0.0001, E-value < 0.05 and q-value < 0.05) with sequences that contained differentially methylated CpG loci in cells treated with 22:6n-3 and/or 18:1n-9. These pTREs included members of the Kruppel-like factor family, the specificity protein family and zinc finger proteins (Table 3). Twelve pTREs were aligned with sequences containing differentially methylated CpG loci in cells treated with 22:6n-3, two pTREs were aligned with differentially methylated CpGs in cells treated with 18:1n-9, and the remaining thirteen pTREs were associated with differentially methylated CpG loci in cells treated with either fatty acid. 22/27 of the pTREs that were identified interact with transcription factors that contain a zinc finger type Cys2-His2 DNA binding domain (Table 3). There did not appear to be any simple pattern of association between fatty acid treatment and the nature of the DNA binding domain of proteins that bind to the PTREs that were associated with differentially methylated CpG loci (Table 3). The PPARα response element was not aligned significantly with differentially methylated CpGs.

4. Discussion

Together these findings showed that incubation with either 22:6n-3 and 18:1n-9 at a physiologically relevant concentration can induce CpG locus-specific changes in DNA methylation in Jurkat cells that were contingent on the type of fatty acid. Such differentially methylated CpG loci were enriched in intergenic regions and were aligned with pTREs for several transcription factors, some of which distinguished between treatment with 22:6n-3 and those treated with 18:1n-9.

As expected, incubation with either 22:6n-3 or 18:1n-9 increased the proportions of these fatty acids in fatty acids in Jurkat cells. The increased proportions of 22:5n-3, 20:5n-3 and 20:3n-3 in cells treated with 22:6n-3 suggests retro-conversion of 22:6n-3 to shorter chain, less unsaturated fatty acids by the pathway reported previously to involve peroxisomal fatty acid β-oxidation [29, 30]. The increase in the proportion of 20:1n-9 in cells treated with 18:1n-9 is consistent with chain elongation of this fatty acid. The increase in the proportions of saturated and monounsaturated fatty acids in cells treated with 22:6n-3 may have been due fatty acid β-oxidation and carbon recycling via fatty acid synthesis *de novo* [31], while the reciprocal changes in the proportions of 16:0 and 16:1n-7 suggest feedback inhibition of Δ9 desaturase by 18:1n-9.

The Illumina 850K array was used to provide the widest coverage of the effects of fatty acids on the DNA methylome reported to date. The changes in DHA methylation that were detected by the array were validated by pyrosequencing. Experiments in humans [5, 6, 32]. animal models [3, 4, 33], and in cultured cells [7, 9] have suggested that, based on analysis of candidate genes or lower coverage DNA methylation arrays, fatty acids can induce differential changes in the methylation status of individual CpG loci and that the pattern of such changes is related to the fatty acid treatment. The present findings support this view by showing that treatment with 22:6n-3 induced a change in methylation status of almost three-fold more CpG loci than were altered by 18:1n-9 treatment while the methylation status of only 78 loci was changed with both fatty acids. This agrees with the findings of a study in which THP-1 cells were incubated with either arachidonic acid (20:4n-3) or 18:1n-9 in that the number of altered CpG loci was greater in cells treated with 20:4n-6 than those incubated with 18:1n-9 [9], and also with *in vivo* dietary modification studies in humans [5] and rodents [4]. The present findings show that 22:6n-3 tended to induce a smaller proportion of hypermethylated loci than 18:1n-9 in Jurkat cells, while 20:4n-4 had a greater tendency to increase the methylation status of CpG loci compared to 18:1n-9 in THP-1 cells [9]. The intergenic > genic distribution of altered CpG loci may indicate that fatty acids may preferentially alter DNA methylation in DNA regulatory elements than coding regions.

The pathways that were most enriched for altered CpGs differed markedly between Jurkat cells treated with 22:6n-3 and those treated with 18:1n-9. Pathways enriched with altered CpGs in

cells treated with 22:6n-3 included two related to the cancer phenotype, namely Netrin Signalling [34] and Protein Kinase A Signalling [35] which may be consistent with reported effects of 22:6n-3 on cancer cells [36]. The possible functional significance in leukaemia cells of enrichment of pathways involved in axonal growth and signalling cannot be easily deduced based on current knowledge. The pathways enriched in differentially methylated CpG loci in cells treated with 18:1n-9 were primarily involved in trans-membrane cell signalling and cell differentiation. Overall, current and previous findings suggest that although a range of fatty acids can alter DNA methylation, capacity of PUFA to alter the DNA methylome appears to be greater than for other fatty acid classes, although such effects may differ between cell types.

Previous studies of the effect of fatty acids on DNA methylation in cultured cells used incubation periods of 24 hours [7, 9, 37]. The present findings show that there was no statistically significant change in DNA methylation of the five candidate loci in cells treated with 22:6n-3 before 72 hours. This suggests that the changes in DNA methylation induced by fatty acids may be a multi-step or multi-factor process. For example, increased methylation requires recruitment of a DNA methyltransferase (DNMT) [37, 38]. Active demethylation has been suggested to involve the activities of several enzymes including ten-eleven translocases (TET) [39-41], methyl binding domain protein (MBD)2b [42], MBD4 [43], the DNA repair endonuclease XPG (Gadd45a) [44] and a G/T mismatch repair DNA glycosylase [45]. PPARα has been implicated in mediating the effects of 20:4n-3 on DNA methylation in THP-1 monocytes, while PPARγ has been shown to interact with TET2[46]. Thus, it possible that members of the PPAR family of fatty acid-binding transcription factors may be involved in targeting of TET activity to specific CpG loci, although it is currently not known whether PPARα can interact with TET proteins. PPARα can act with DNMT1 [47], but the mechanism of this interaction is not known. Thus, it is plausible that PPARs may have a role in mediating the targeting of DNA methyltransferase and/or DNA demethylase activity to individual CpG loci. However, the present study did not find evidence of the involvement of PPARα in mediating the effects of 22:6n-3 on DNA methylation in five candidate loci. Instead, several pTREs were identified that aligned with DNA sequencings which were proximal to differentially methylated CpG loci. The majority of these pTREs interact with transcription factors that contain zinc-finger DNA binding domains. This suggests that zinc-finger proteins are involved in targeting fatty acid-induced changes in DNA methylation to specific loci, although it is also possible that this observation may reflect the abundance of these DNA binding motifs in the human proteome [48]. Moreover, WT1 been shown to recruit Tet2 to its response element in HL60 cells [49] and SP1 has shown to interact with DNMT1 in HEK293 cells [50].

Thus, it is possible that WT1 and SP1 may facilitate targeting of DNA methyltransferase or demethylase activities to specific CpG loci.

5. CONCLUSIONS

Overall, these findings show that incubation with 22:6n-3 or 18:1n-9 induced CpG locus-specific DNA methylation changes in Jurkat cells which occurred over different periods time contingent on the CpG locus. Differentially methylated CpG loci were associated with pTREs which may provide a mechanism for mediating locus-specific changes in DNA methylation by fatty acids. Since differential methylation of individual CpG loci has been shown to predict traits that are associated with risk of cardiometabolic disease [51-54], one implication of the present findings is that it may be possible to develop dietary interventions based on specific combinations of fatty acids to modify the methylation status of disease-associated CpG loci.

ACKNOWLEDGEMENTS

We wish to thank Dr Michael Kobor's group at the Centre for Molecular Medicine and Therapeutics, British Columbia Children's Research Hospital Institute, University of British Columbia, Vancouver, Canada for carrying out the 850K methylation array hybridisation.

AUTHOR CONTRIBUTIONS

GCB and KAL designed the study and, together with CC and PCC, supervised the work. JEP-M carried out the experiments and analysed the data. GCB and JEP-M wrote the manuscript with input from all authors.

AUTHOR DECLARATIONS

GCB has received research funding from Nestle, Abbott Nutrition and Danone. He has served as member of the Scientific Advisory Board of BASF and is member of the BASF Asia Grant Panel. PCC acts as a consultant to BASF AS, Cargill, Smartfish, DSM and Fresenius-Kabi. The authors state they have no conflicts of interest related to the work presented in this manuscript. None of the other authors has disclosures or conflicts of interest to report.

References

[1] G.C. Burdge, Is essential fatty acid interconversion an important source of polyunsaturated fatty acids in humans?, Br J Nutr 27 (2018) 1-28.

[2] G.C. Burdge, K.A. Lillycrop, Fatty acids and epigenetics, Current opinion in clinical nutrition and metabolic care, 17 (2014) 156-161.

[3] M.D. Niculescu, D.S. Lupu, C.N. Craciunescu, Perinatal manipulation of alpha-linolenic acid intake induces epigenetic changes in maternal and offspring livers, FASEB J 27 (2013) 350-358.

[4] S.P. Hoile, N.A. Irvine, C.J. Kelsall, et al. Maternal fat intake in rats alters 20:4n-6 and 22:6n-3 status and the epigenetic regulation of Fads2 in offspring liver, The Journal of nutritional biochemistry, (2012).

[5] S.P. Hoile, R. Clarke-Harris, R.C. Huang, *et al.* Supplementation with n-3 Long-Chain Polyunsaturated Fatty Acids or Olive Oil in Men and Women with Renal Disease Induces Differential Changes in the DNA Methylation of FADS2 and ELOVL5 in Peripheral Blood Mononuclear Cells, PLoS One, 9 (2014) e109896.

[6] S.J. van Dijk, J. Zhou, T.J. Peters, *et al.* Effect of prenatal DHA supplementation on the infant epigenome: results from a randomized controlled trial, Clin Epigenetics, 8 (2016) 114.

[7] V. Ceccarelli, S. Racanicchi, M.P. Martelli, *et al.*, Eicosapentaenoic acid demethylates a single CpG that mediates expression of tumor suppressor CCAAT/enhancer-binding protein delta in U937 leukemia cells, Journal of Biological Chemistry, 286 (2011) 27092-27102.

[8] V. Ceccarelli, G. Nocentini, M. Billi, *et al.* Eicosapentaenoic acid activates RAS/ERK/C/EBPbeta pathway through H-Ras intron 1 CpG island demethylation in U937 leukemia cells, PLoS One, 9 (2014) e85025.

[9] G.A. Silva-Martinez, D. Rodriguez-Rios, Y. Alvarado-Caudillo, *et al.*, Arachidonic and oleic acid exert distinct effects on the DNA methylome, Epigenetics, 11 (2016) 321-334.

[10] A.L. West, E.A. Miles, K.A. Lillycrop, *et al.*, Postprandial incorporation of EPA and DHA from transgenic Camelina sativa oil into blood lipids is equivalent to that from fish oil in healthy humans, Br J Nutr, (2019) 1-27.

[11] A.L. West, G.C. Burdge, P.C. Calder, Lipid structure does not modify incorporation of EPA and DHA into blood lipids in healthy adults: a randomised-controlled trial, Br J Nutr, 116 (2016) 788-797.

[12] J. Folch, M. Lees, G.H. Sloane Stanley, A simple method for the isolation and purification of total lipides from animal tissues, J Biol Chem, 226 (1957) 497-509.

[13] R. Pidsley, E. Zotenko, T.J. Peters, *et al.*, Critical evaluation of the Illumina MethylationEPIC BeadChip microarray for whole-genome DNA methylation profiling, Genome Biol, 17 (2016) 208.

[14] M.J. Aryee, A.E. Jaffe, H. Corrada-Bravo, C. *et al.*, Minfi: a flexible and comprehensive Bioconductor package for the analysis of Infinium DNA methylation microarrays, Bioinformatics, 30 (2014) 1363-1369.
[15] J. Maksimovic, B. Phipson, A. Oshlack, A cross-package Bioconductor workflow for analysing methylation array data, F1000Res, 5 (2016) 1281.
[16] Y.A. Chen, M. Lemire, S. Choufani, *et al.*, Discovery of cross-reactive probes and polymorphic CpGs in the Illumina Infinium HumanMethylation450 microarray, Epigenetics, 8 (2013) 203-209.
[17] J.P. Fortin, A. Labbe, M. Lemire, *et al.*, Functional normalization of 450k methylation array data improves replication in large cancer studies, Genome Biol, 15 (2014) 503.
[18] W.E. Johnson, C. Li, A. Rabinovic, Adjusting batch effects in microarray expression data using empirical Bayes methods, Biostatistics, 8 (2007) 118-127.
[19] Y. Benjamini, Y. Hochberg, Controlling the False Discovery Rate - a Practical and Powerful Approach to Multiple Testing, J Roy Stat Soc B Met, 57 (1995) 289-300.
[20] S.P. Hoile, N.A. Irvine, C.J. Kelsall, C. *et al.*, Maternal fat intake in rats alters 20:4n-6 and 22:6n-3 status and the epigenetic regulation of Fads2 in offspring liver, J Nutr Biochem, 24 (2013) 1213-1220.
[21] C.M. Sibbons, N.A. Irvine, J.E. Perez-Mojica, *et al.*, Polyunsaturated Fatty Acid Biosynthesis Involving Delta 8 Desaturation and Differential DNA Methylation of FADS2 Regulates Proliferation of Human Peripheral Blood Mononuclear Cells, Front Immunol, 9 (2018) 432.
[22] A.J. Stewart, S. Hannenhalli, J.B. Plotkin, Why transcription factor binding sites are ten nucleotides long, Genetics, 192 (2012) 973-985.
[23] T.L. Bailey, C. Elkan, Fitting a mixture model by expectation maximization to discover motifs in biopolymers, Proc Int Conf Intell Syst Mol Biol, 2 (1994) 28-36.
[24] S. Heinz, C. Benner, N. Spann, *et al.* Glass, Simple combinations of lineage-determining transcription factors prime cis-regulatory elements required for macrophage and B cell identities, Mol Cell, 38 (2010) 576-589.
[25] S. Mahony, P.E. Auron, P.V. Benos, DNA familial binding profiles made easy: Comparison of various motif alignment and clustering strategies, Plos Comput Biol, 3 (2007) 578-591.
[26] S. Mahony, P.V. Benos, STAMP: a web tool for exploring DNA-binding motif similarities, Nucleic Acids Research, 35 (2007) W253-W258.
[27] S. Gupta, J.A. Stamatoyannopoulos, T.L. Bailey, W.S. Noble, Quantifying similarity between motifs, Genome Biology, 8 (2007).

[28] I.V. Kulakovskiy, I.E. Vorontsov, I.S. Yevshin, *et al.* et al, HOCOMOCO: towards a complete collection of transcription factor binding models for human and mouse via large-scale ChIP-Seq analysis, Nuc Acids Research, 46 (2018) D252-D259.
[29] W. Stoffel, Eker, H. Assad, H. Sprecher, Enzymatic studies on the mechanism of the retroconversion of C22-polyenoic fatty acids to their C20-homologues, Hoppe Seylers Z Physiol Chem, 351 (1970) 1545-1554.
[30] E. Christensen, B. Woldseth, T.A. Hagve, B.T. *et al.*, Peroxisomal beta-oxidation of polyunsaturated long chain fatty acids in human fibroblasts. The polyunsaturated and the saturated long chain fatty acids are retroconverted by the same acyl-CoA oxidase, Scand J Clin Lab Invest Suppl, 215 (1993) 61-74.
[31] G.C. Burdge, S.A. Wootton, Conversion of alpha-linolenic acid to palmitic, palmitoleic, stearic and oleic acids in men and women, Prostaglandins Leukot.Essent.Fatty Acids, 69 (2003) 283-290.
[32] S.C. Jacobsen, C. Brons, J. Bork-Jensen, *et al.*, Effects of short-term high-fat overfeeding on genome-wide DNA methylation in the skeletal muscle of healthy young men, Diabetologia, 55 (2012) 3341-3349.
[33] C.J. Kelsall, S.P. Hoile, N.A. Irvine, *et al.*, G.C. Burdge, Vascular dysfunction induced in offspring by maternal dietary fat involves altered arterial polyunsaturated Fatty Acid biosynthesis, PLoS One, 7 (2012) e34492.
[34] H. Arakawa, Netrin-1 and its receptors in tumorigenesis, Nature reviews. Cancer, 4 (2004) 978-987.
[35] A. Caretta, C. Mucignat-Caretta, Protein kinase a in cancer, Cancers (Basel), 3 (2011) 913-926.
[36] M. Newell, K. Baker, L.M. Postovit, C.J. Field, A Critical Review on the Effect of Docosahexaenoic Acid (DHA) on Cancer Cell Cycle Progression, International journal of molecular sciences, 18 (2017).
[37] R. Rangel-Salazar, M. Wickstrom-Lindholm, C.A. Aguilar-Salinas, *et al.*, Human native lipoprotein-induced de novo DNA methylation is associated with repression of inflammatory genes in THP-1 macrophages, BMC genomics, 12 (2011) 582.
[38] M. Okano, D.W. Bell, D.A. Haber, E. Li, DNA methyltransferases Dnmt3a and Dnmt3b are essential for de novo methylation and mammalian development, Cell, 99 (1999) 247-257.
[39] S. Ito, A.C. D'Alessio, O.V. Taranova, K. Hong, L.C. Sowers, Y. Zhang, Role of Tet proteins in 5mC to 5hmC conversion, ES-cell self-renewal and inner cell mass specification, Nature, 466 (2010) 1129-1133.
[40] M. Tahiliani, K.P. Koh, Y. Shen, *et al.*, Conversion of 5-methylcytosine to 5-hydroxymethylcytosine in mammalian DNA by MLL partner TET1, Science, 324 (2009) 930-935.

[41] V. Ceccarelli, V. Valentini, S. Ronchetti, *et al.*, Vecchini, Eicosapentaenoic acid induces DNA demethylation in carcinoma cells through a TET1-dependent mechanism, FASEB J, (2018) fj201800245R.
[42] S.K. Bhattacharya, S. Ramchandani, N. Cervoni, M. Szyf, A mammalian protein with specific demethylase activity for mCpG DNA, Nature, 397 (1999) 579-583.
[43] B. Zhu, Y. Zheng, H. Angliker, *et al.*, 5-Methylcytosine DNA glycosylase activity is also present in the human MBD4 (G/T mismatch glycosylase) and in a related avian sequence, Nucleic Acids Res, 28 (2000) 4157-4165.
[44] G. Barreto, A. Schafer, J. Marhold, *et al.*, Gadd45a promotes epigenetic gene activation by repair-mediated DNA demethylation, Nature, 445 (2007) 671-675.
[45] J.P. Jost, Nuclear Extracts of Chicken Embryos Promote An Active Demethylation of Dna by Excision Repair of 5-Methyldeoxycytidine, Proc Natl Acad Sci USA, 90 (1993) 4684-4688.
[46] F. Bian, X. Ma, S.D. Villivalam, *et al.* TET2 facilitates PPARgamma agonist-mediated gene regulation and insulin sensitization in adipocytes, Metabolism, 89 (2018) 39-47.
[47] Y. Luo, C. Xie, C.N. Brocker, *et al.*, Intestinal PPARalpha Protects Against Colon Carcinogenesis via Regulation of Methyltransferases DNMT1 and PRMT6, Gastroenterology, 157 (2019) 744-759 e744.
[48] N.O. Hudson, B.A. Buck-Koehntop, Zinc Finger Readers of Methylated DNA, Molecules, 23 (2018).
[49] Y. Wang, M. Xiao, X. Chen, *et al.*, WT1 recruits TET2 to regulate its target gene expression and suppress leukemia cell proliferation, Mol Cell, 57 (2015) 662-673.
[50] P.O. Esteve, H.G. Chin, S. Pradhan, Molecular mechanisms of transactivation and doxorubicin-mediated repression of survivin gene in cancer cells, Journal of Biological Chemistry, 282 (2007) 2615-2625.
[51] R. Clarke-Harris, T.J. Wilkin, J. Hosking, *et al.*, Peroxisomal proliferator activated receptor-gamma-co-activator-1alpha promoter methylation in blood at 5-7 years predicts adiposity from 9 to 14 years (EarlyBird 50), Diabetes, (2014).
[52] K.M. Godfrey, A. Sheppard, P.D. Gluckman, *et al.*, Epigenetic gene promoter methylation at birth is associated with child's later adiposity, Diabetes, 60 (2011) 1528-1534.
[53] K. Lillycrop, R. Murray, C. Cheong, *et al.*, ANRIL Promoter DNA Methylation: A Perinatal Marker for Later Adiposity, EBioMedicine, 19 (2017) 60-72.
[54] R. Murray, J. Bryant, P. Titcombe, *et al.*, DNA methylation at birth within the promoter of ANRIL predicts markers of cardiovascular risk at 9 years, Clin Epigenetics, 8 (2016) 90.

Table 1. PCR and Pyrosequencing primers

850K CpG ID	Primer Sequences (5'-3')	Temp[a] (ºC)	Size[b] (bp)
cg26292058	Fwd TGTATATATTTGATAGGAGGGAAAGT Rev BIO-ACACCCCTTAAAATCATCCTATATATTAC Seq TTTAAGGTGTGTGTTAGA	57	162
cg05475386	Fwd GTGTTTTTTGAGAGGAAATGGGTGATAAT Rev BIO-TACATTACACAAACCTTATTAAACATTACC Seq GGTTTTTTAATAGAAGGA	57	121
cg27188282	Fwd AGGGTAAAGTTTGAGGGTATTTGT Rev BIO-ATCTTCTTCCCAAAACATCTTCTC Seq TGTTTTTGTGATTTAATTTATTATTTAAG	62	165
cg06989443	Fwd BIO-TTAGGTAGATGGGGGAGTTGG Rev ACAAACAAACAAATAATTCCCCCTTACA Seq CTAAAAACAACTATTTATTCCCT	57	246
cg22518417	Fwd BIO-TTTTGTTATTATTTAGATTGTGGTTTGG Rev ACCCAACCTTCTAATCTTTTCATAA Seq AAAAAACATTAATACTTATATACT	57	79

Fwd, forward primer; Rev, reverse primer; Seq, sequencing primer; BIO-, biotin-labeled primer.

[a]Annealing temperature; [b]Amplicon size.

Table 2. Top ten canonical pathways enriched for differentially methylated genes.

		Number of differentially methylated loci		
		Methylation change		Number of
IPA® Canonical Pathways	P	Increased	Decreased	genes
Pathways altered by incubation with 22:6n-3				
Synaptic Long-Term Potentiation	<0.0001	7	12	17
Synaptic Long-Term Depression	<0.0001	5	17	20
Protein Kinase A Signalling	0.0001	12	29	34
Netrin Signalling	0.0001	4	7	11
Dopamine-PPP1R1B Feedback in cAMP Signalling	0.0002	8	10	18
GPCR-Mediated Integration of Enteroendocrine Signalling	0.0003	3	8	11
Axonal Guidance Signalling	0.0003	17	21	36
G Protein Signalling Mediated by Tubby	0.0003	4	3	7
GPCR-Mediated Nutrient Sensing in Enteroendocrine Cells	0.0003	4	10	14
Cellular Effects of Sildenafil	0.0004	5	15	15
Pathways altered by incubation with 18:1n-9				
Amyotrophic Lateral Sclerosis Signalling	0.0005	4	4	8
Opioid Signalling Pathway	0.0065	5	5	10
Aryl Hydrocarbon Receptor Signalling	0.0076	3	6	9
Clathrin-mediated Endocytosis Signalling	0.0076	5	4	7
Human Embryonic Stem Cell Pluripotency	0.0089	3	4	7
Fcγ Receptor IIB Signalling in B Lymphocytes	0.0100	4	1	5
Glioma Signalling	0.0115	5	2	6
Regulation of the Epithelial-Mesenchymal Transition	0.0129	4	4	8
Retinoate Biosynthesis I	0.0145	2	1	3
Pigment Epithelium-derived Factor (PEDF) Signalling	0.0145	3	2	5

P-values were calculated using Fisher's exact test for Canonical pathways function in IPA®. PPP1R1B, protein phosphatase 1 Regulatory subunit 1B; cAMP, cyclic adenosine monophosphate; GPCR, g-protein-coupled receptors.

Table 3. Putative transcription factor response elements enriched at differentially methylated CpG loci in Jurkat cells treated with 22:6n-3 or 18:1n-9.

Name	Symbol	DNA binding domains[a]	Treatment
Androgen receptor	AR	ZF-C4	22:6n-3[c]
Early growth response 1	EGR1	ZF-C2H2	22:6n-3[b]
Forkhead box J3	FOXJ3	Fork-head	22:6n-3[c]
IKAROS family zinc finger 1	IKZF1	ZF-C2H2	22:6n-3[b]
Kruppel-like factor 1	KLF1	ZF-C2H2	22:6n-3[b]
Kruppel-like factor 3	KLF3	ZF-C2H2	22:6n-3[a] and 18:1n-9[a]
Kruppel-like factor 15	KLF9	ZF-C2H2	18:1n-9[d]
Kruppel-like factor 15	KLF15	ZF-C2H2	22:6n-3[a] and 18:1n-9[d]
MYC associated zinc finger protein	MAZ	ZF-C2H2	22:6n-3[ab] and 18:1n-9[a]
POZ/BTB and AT hook containing zinc finger 1	PATZ1	A.T. hook, ZF-C2H2	22:6n-3[ab] and 18:1n-9[a]
PR/SET domain 6	PRDM6	ZF-C2H2	22:6n-3[c]
Sp1 transcription factor	SP1	ZF-C2H2	22:6n-3[ab] and 18:1n-9[a]
Sp2 transcription factor	SP2	ZF-C2H2	22:6n-3[ab] and 18:1n-9[a]
Sp3 transcription factor	SP3	ZF-C2H2	22:6n-3[ab] and 18:1n-9[ab]
Sp4 transcription factor	SP4	ZF-C2H2	22:6n-3[a]
Sex determining region Y	SRY	HMG box	22:6n-3[c]
TATA-box binding protein associated factor 1	TAF1	HMG box	22:6n-3[a]
Upstream transcription factor 2, C-fos interacting	USF2	bHLH and L-Z	18:1n-9[a]
Vascular endothelial zinc finger 1	VEZF1	ZF-C2H2	22:6n-3[ab] and 18:1n-9[d]
Wilms tumour 1	WT1	ZF-C2H2	22:6n-3[b] and 18:1n-9[ab]
Zinc finger and BTB domain containing 17	ZBT17	ZF-C2H2	22:6n-3[a]
Zinc finger protein 250	ZN250	ZF-C2H2	22:6n-3[bd]
Zinc finger protein 263	ZN263	ZF-C2H2	22:6n-3[a]
Zinc finger protein 281	ZN281	ZF-C2H2	22:6n-3[a] and 18:1n-9[a]
Zinc finger protein 341	ZN341	ZF-C2H2	22:6n-3[a] and 18:1n-9[d]

Zinc finger protein 467	ZN467	ZF-C2H2	22:6n-3[ab] and 18:1n-9[a]
Zinc finger protein 770	ZN770	ZF-C2H2	22:6n-3[a] and 18:1n-9[b]

Superscripts indicate that alignment was identified using differentially methylated DNA sequences in [a], any genomic region; [b], intergenic regions; [c], promoter regions; or [d], gene body regions. ZF-C4, zinc finger type Cys4; ZF-C2H2, zinc finger type Cys2-His2; A.T. hook, adenine-thymine hook; HMG box, high mobility group box; bHLH, basic helix-loop-helix; L-Z, leucine-zipper. [a]Data from UniProt Knowledgebase (UniProtKB). Only manually annotated records extracted from literature with further computational analysis were used.

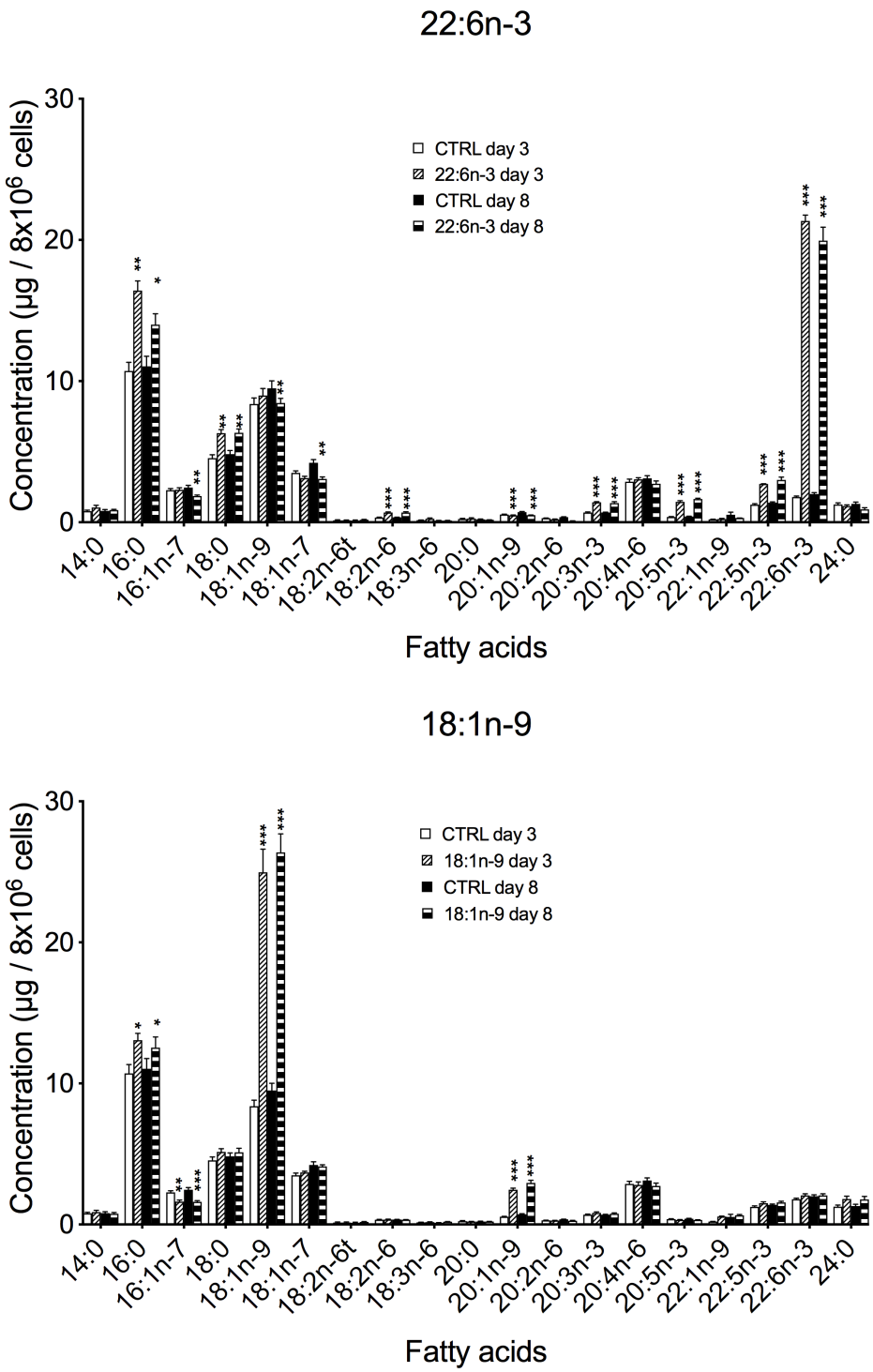

Figure 1. Fatty acid composition of Jurkat cells before and after treatment for 3 (n = 4 replicate cultures) or 8 days (n = 7 replicate cultures) with 15 µM either 22:6n-3 or 18:1n-9. Data are mean ± standard error of the mean. Control versus treatment means at each time point were compared by Student's unpaired t-test. Means that differed significantly between cells treated with 22:6n-3 or 18:1n-9 are indicated by *P < 0.05, **P < 0.01 and ***P < 0.001.

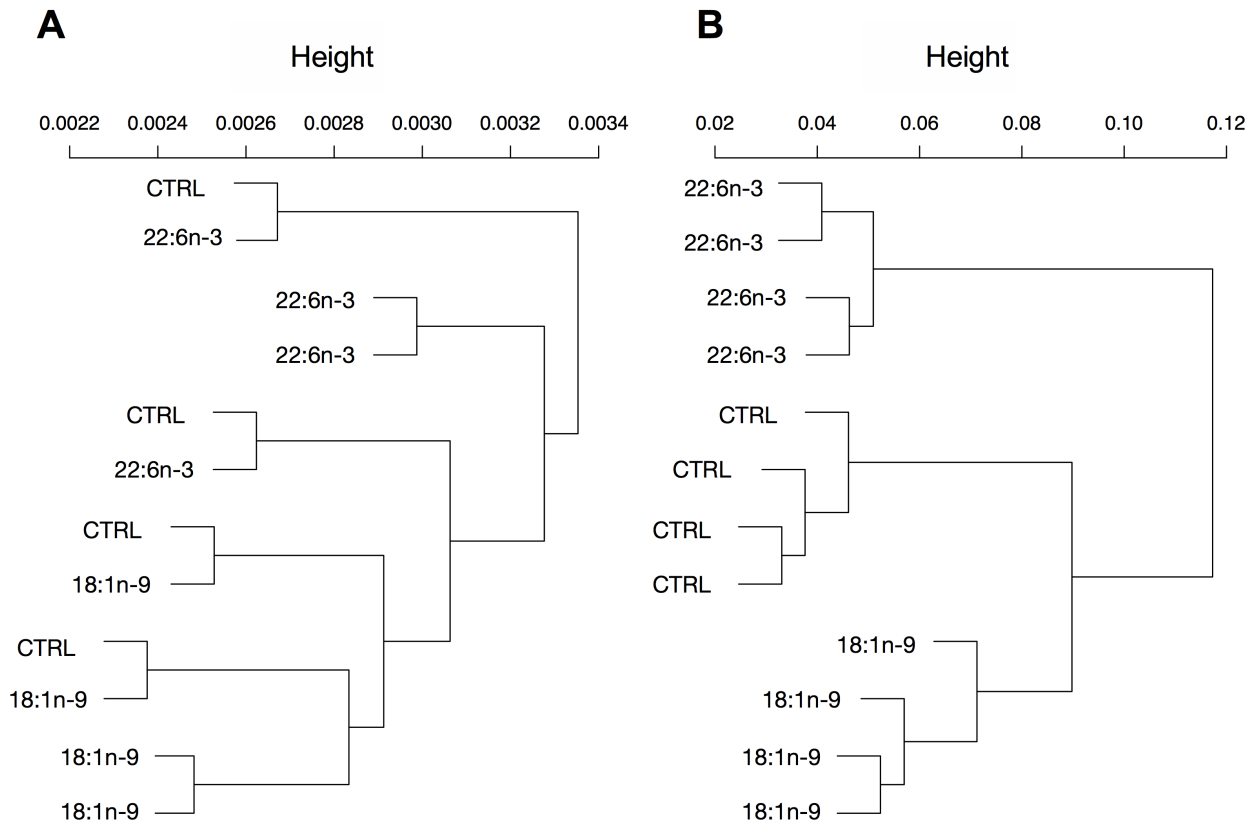

Figure 2. Cluster dendrogram of samples (n = 4 culture replicates per treatment). (A) Unsupervised clustering of M-values of all CpG loci analysed in the 850K array. (B) Unsupervised clustering of M-values of differentially methylated CpG loci only.

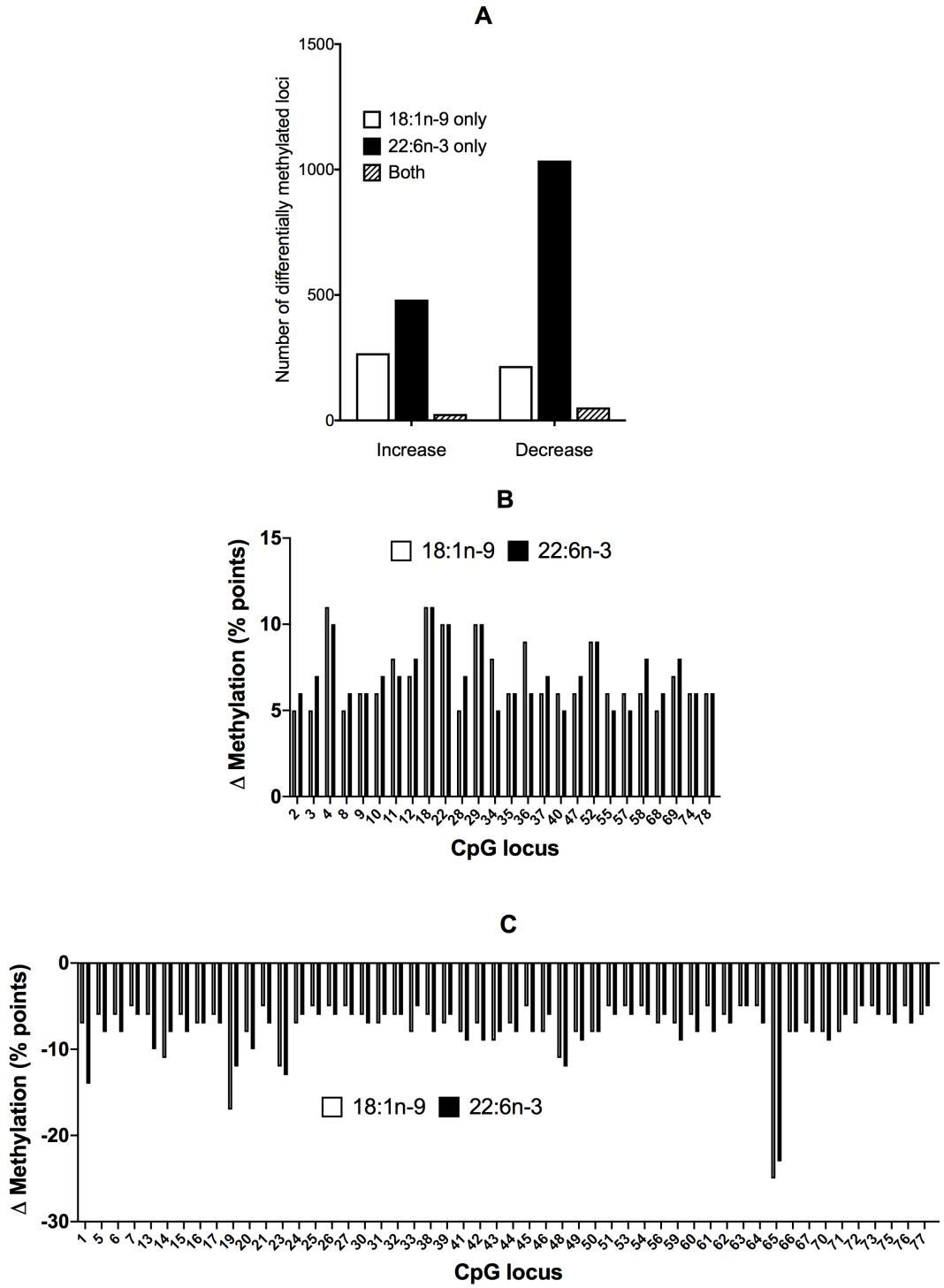

Figure 3. Number and direction of change of differentially methylated CpG loci after treatment with 22:6n-3 or 18:1n-9 for 8 days. (A) Total number of differentially methylated CpG loci. (B) Change in methylation of loci hypermethylated compared to vehicle control by 22:6n-3 or 18:1n-9. (C) Change in methylation of loci hypomethylated compared to vehicle control by 22:6n-3 or 18:1n-9. The chromosome locations of the differentially methylated CpG loci are shown in Supplemental Table 2.

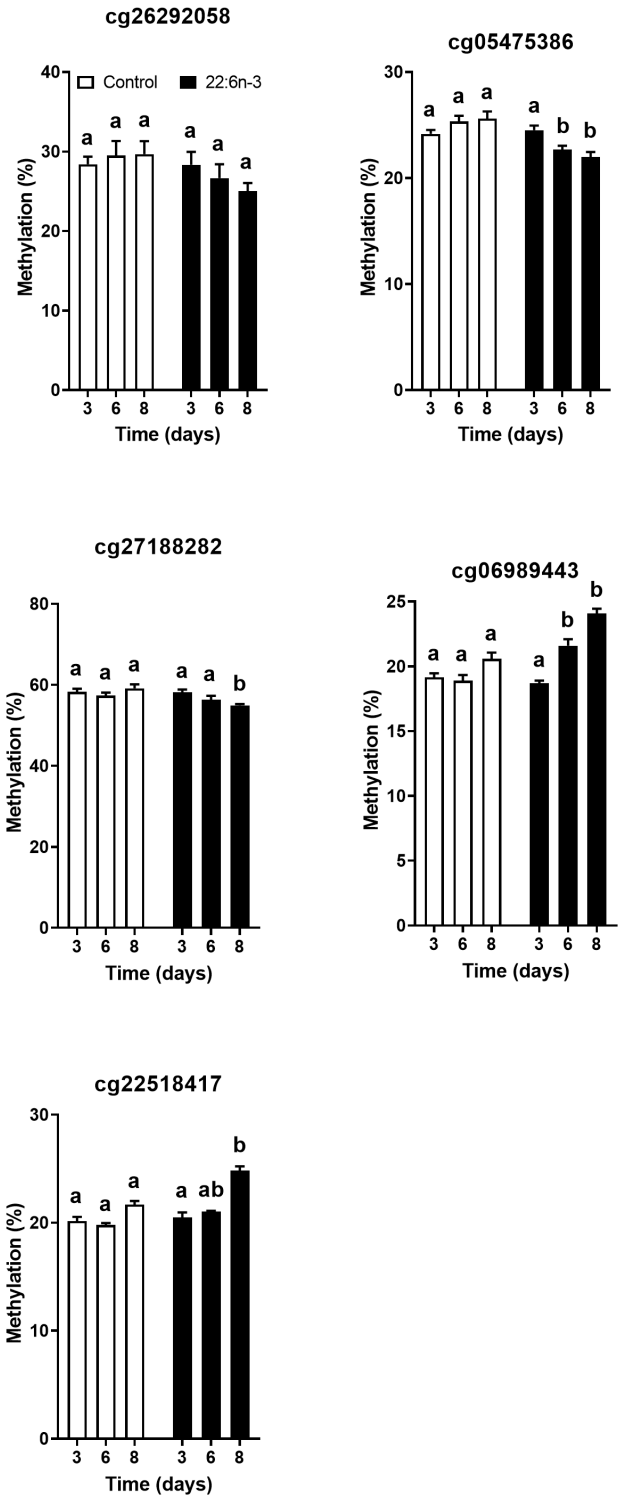

Fig. 4. Methylation status of candidate CpG loci after 3 (n = 8), 6 (n = 8) and 8 (n = 6) days incubation with 22:6n-3. Data are shown as means ± SEM. Statistical comparisons were by two-way ANOVA with Tukey *post-hoc* test. Means that differed significantly ($P<0.05$) between timepoints are indicated by different letters.

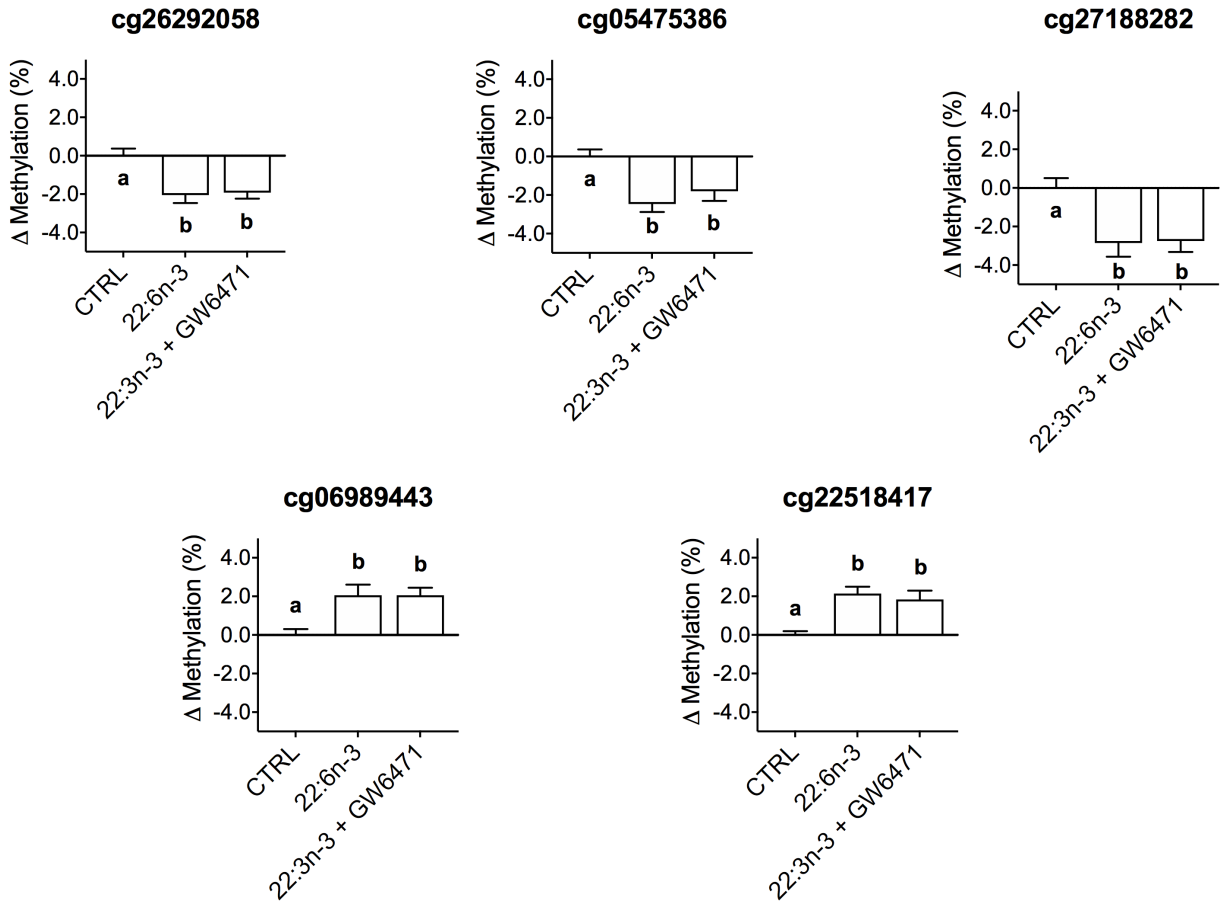

Fig. 5. The effect of the PPARα antagonist GW6471 on the induction of altered DNA methylation of 5 candidate CpG loci by 22:6n-3. Values are mean ± SEM change in DNA methylation after incubation for 8 days with either vehicle (CTRL, control) or 22:6n-3 alone, or 22:6n-3 plus GW6471. CpG loci are indicated by their chromosome locations. Means were compared by 1-way ANOVA with Tukey's post hoc test for multiple comparisons. Means which differed significantly ($P<0.05$) are indicated by different letters.

Supplemental Online Material

Pérez-Mojica, Lillycrop, Cooper, Calder, Burdge

Docosahexaenoic acid and oleic acid induce altered DNA methylation of individual CpG loci in Jurkat T cells

Supplemental Table 1. DNA methylation of CpG loci that were altered by 22:6n-3 and 18:1n-9.

CpG Number	IlmnID	Chr	Chr Position	Strand	CpGi	Gene	Gene Region	22:6n-3 (Δ% pts)	18:1n-9 (Δ% pts)
1	cg26292058	1	192544252	-	OpenSea	RGS1	TSS1500	-14.0%	-7.0%
2	cg23243552	1	98500398	-	OpenSea	MIR137HG	Body	6.0%	5.0%
3	cg17002156	1	183995878	+	OpenSea	GLT25D2	Body	7.0%	5.0%
4	cg17291907	1	47010131	+	Island	no gene	no gene	10.0%	11.0%
5	cg24042978	2	167344458	-	OpenSea	SCN7A	TSS1500	-8.0%	-6.0%
6	cg27301645	2	88667670	+	OpenSea	no gene	no gene	-8.0%	-6.0%
7	cg14383480	2	168043663	-	OpenSea	XIRP2	Body	-6.0%	-5.0%
8	cg15355298	2	48011201	-	Island	MSH6	Body	6.0%	5.0%
9	cg18946478	2	20866414	-	Island	GDF7	TSS200	6.0%	6.0%
10	cg24203562	2	239241869	+	OpenSea	TRAF3IP1	Body	7.0%	6.0%
11	cg26001287	2	111877753	-	Island	BCL2L11	TSS1500	7.0%	8.0%
12	ch.2.252555R*	2	9381833	+	OpenSea	ASAP2	Body	8.0%	7.0%
13	cg17420463	3	185046594	-	OpenSea	MAP3K13	NC	-10.0%	-6.0%
14	cg15237829	3	171102373	+	OpenSea	TNIK	Body	-8.0%	-11.0%
15	cg05401575	3	63428587	-	OpenSea	SYNPR	NC	-8.0%	-6.0%

16	cg21195620	3	15838030	-	OpenSea	ANKRD28	NC	-7.0%	-7.0%
17	cg12405098	3	178275369	-	OpenSea	KCNMB2	NC	-7.0%	-6.0%
18	cg04730456	3	122510658	-	N_Shore	HSPBAP1	Body	11.0%	11.0%
19	cg10841253	4	10531768	+	OpenSea	CLNK	Body	-12.0%	-17.0%
20	cg07321467	4	81960704	-	OpenSea	BMP3	Body	-10.0%	-8.0%
21	cg07815324	4	43135729	-	OpenSea	no gene	no gene	-7.0%	-5.0%
22	cg17089062	4	174427773	-	N_Shore	no gene	no gene	10.0%	10.0%
23	cg04574083	5	6765204	-	OpenSea	no gene	no gene	-13.0%	-12.0%
24	cg03701805	5	122452418	+	OpenSea	PRDM6	Body	-6.0%	-7.0%
25	cg19508967	5	1840347	+	OpenSea	no gene	no gene	-6.0%	-5.0%
26	cg03570708	5	133135701	+	OpenSea	no gene	no gene	-6.0%	-5.0%
27	cg18052369	5	99970791	+	OpenSea	no gene	no gene	-6.0%	-5.0%
28	cg26092471	5	174150712	+	N_Shore	MSX2	TSS1500	7.0%	5.0%
29	cg00417638	5	5586070	-	OpenSea	no gene	no gene	10.0%	10.0%
30	cg13396038	6	141766970	-	OpenSea	no gene	no gene	-7.0%	-6.0%
31	cg09160330	6	46760919	-	OpenSea	MEP1A	TSS200	-6.0%	-7.0%
32	cg15416661	6	28725789	-	OpenSea	no gene	no gene	-6.0%	-6.0%
33	cg27639249	6	30016420	+	OpenSea	NCRNA00171	Body	-5.0%	-8.0%
34	cg05938671	6	125421084	-	Island	no gene	no gene	5.0%	8.0%
35	cg22170402	6	76553236	+	OpenSea	MYO6	Body	6.0%	6.0%
36	cg06423354	6	30165652	+	OpenSea	TRIM26	Body	6.0%	9.0%
37	cg08760395	6	53275751	+	OpenSea	no gene	no gene	7.0%	6.0%
38	cg19878120	7	105655497	-	OpenSea	CDHR3	Body	-8.0%	-6.0%

39	cg00226689	7	41259421	-	OpenSea	no gene	no gene	-6.0%	-7.0%
40	cg24471726	7	90872375	+	OpenSea	no gene	no gene	5.0%	6.0%
41	cg21548021	8	15873055	+	OpenSea	no gene	no gene	-9.0%	-8.0%
42	cg00947236	8	29020165	+	OpenSea	KIF13B	Body	-9.0%	-7.0%
43	cg08997191	8	133788834	-	S_Shore	PHF20L1	5'UTR	-8.0%	-9.0%
44	cg23019611	8	23458336	-	OpenSea	no gene	no gene	-8.0%	-7.0%
45	cg00659910	8	64617139	-	OpenSea	no gene	no gene	-8.0%	-5.0%
46	cg15423200	8	52589863	-	OpenSea	PXDNL	Body	-6.0%	-8.0%
47	cg16467757	8	95888145	+	OpenSea	INTS8	Body	7.0%	6.0%
48	cg05147200	9	22446830	-	Island	DMRTA1	TSS200	-12.0%	-11.0%
49	cg00550721	9	21986062	+	N_Shelf	CDKN2A	Body	-9.0%	-8.0%
50	cg06819082	9	16726627	-	N_Shore	BNC2	Body	-8.0%	-8.0%
51	cg01266362	9	98265802	-	N_Shelf	PTCH1	5'UTR	-6.0%	-5.0%
52	cg05211356	9	19408000	+	N_Shore	ACER2	TSS1500	9.0%	9.0%
53	cg11122255	10	24995583	+	OpenSea	ARHGAP21	Body	-6.0%	-5.0%
54	cg11195065	10	119292371	+	N_Shore	EMX2OS	Body	-6.0%	-5.0%
55	cg23758453	10	48952010	+	N_Shore	NC	NC	5.0%	6.0%
56	cg08531298	11	15515888	-	OpenSea	no gene	no gene	-6.0%	-7.0%
57	cg09721595	11	77773924	-	OpenSea	THRSP	TSS1500	5.0%	6.0%
58	cg10452423	11	116424360	+	OpenSea	no gene	no gene	8.0%	6.0%
59	cg09746078	12	56966920	-	OpenSea	RBMS2	Body	-9.0%	-7.0%
60	cg24907862	12	26112480	-	OpenSea	RASSF8	5'UTR	-8.0%	-6.0%
61	cg07037583	12	72452357	+	OpenSea	no gene	no gene	-8.0%	-5.0%

62	cg19366091	12	44292779	+	OpenSea	TMEM117	Body	-7.0%	-6.0%
63	cg03530940	12	2198113	-	OpenSea	CACNA1C	Body	-5.0%	-5.0%
64	cg14375976	13	29098268	+	OpenSea	no gene	no gene	-7.0%	-5.0%
65	cg02401415	14	22968476	+	OpenSea	no gene	no gene	-23.0%	-25.0%
66	cg26463402	14	74003851	+	N_Shore	HEATR4	5'UTR	-8.0%	-8.0%
67	cg03644541	14	35157273	+	OpenSea	no gene	no gene	-8.0%	-7.0%
68	cg02498946	14	35907902	-	OpenSea	no gene	no gene	6.0%	5.0%
69	cg16908234	16	46835765	+	OpenSea	no gene	no gene	8.0%	7.0%
70	cg03687953	17	40834511	-	N_Shore	NC	NC	-9.0%	-8.0%
71	cg22371052	18	72021321	+	OpenSea	C18orf63	Body	-6.0%	-8.0%
72	cg22542489	21	19616644	-	N_Shore	CHODL	5'UTR	-5.0%	-7.0%
73	cg17016559	22	46067508	+	Island	ATXN10	TSS200	-6.0%	-5.0%
74	cg15383187	22	31344805	+	OpenSea	MORC2	Body	6.0%	6.0%
75	cg20972857	X	47468321	+	OpenSea	SYN1	Body	-7.0%	-6.0%
76	cg23067676	X	40141241	-	OpenSea	LOC101927476	Body	-7.0%	-5.0%
77	cg12705389	X	137794264	+	S_Shore	FGF13	Body	-5.0%	-6.0%
78	cg27515272	X	75648802	+	Island	MAGEE1	1stExon	6.0%	6.0%

CpGi, location of the CpG relative to a CpG island from University of California Santa Cruz (UCSC) database (https://genome.ucsc.edu); Gene region; CpG position within the gene from UCSC database; IlmnID, unique identifier from the Illumina CG database (probe ID); NC, no consensus location; Position, chromosomal coordinates of the CpG from the Genome Reference Consortium Human Build 37 (GRCh37); (Δ% pts), change in methylation (percent points); TSS200, 0-200 bases upstream of the transcription start site (TSS); TSS1500, 200-1500 bases upstream of the TSS. Probe IDs prefixed with indicate non-CpG-targeting probes.

Supplemental Table 2. Validation of 850K array results by pyrosequencing.

	Difference in methylation (%)	
IlmnID	850K Array	Pyrosequencing
cg26292058	-15[a]	-16***
cg05475386	-13[a]	-14**
cg27188282	-11[a]	-7**
cg06989443	12[a]	17***
cg22518417	11[a]	14***

IlmnID, unique identifier from the Illumina CG database. CpG loci were assumed to be differentially methylated at [a]$P < 0.05$ and q-value <0.05. For methylation levels measured by pyrosequencing data, that differed significantly different by Student's unpaired t-test are indicated by *P <0.05, **P<0.01 or P<0.01.

Supplemental Figure 1.

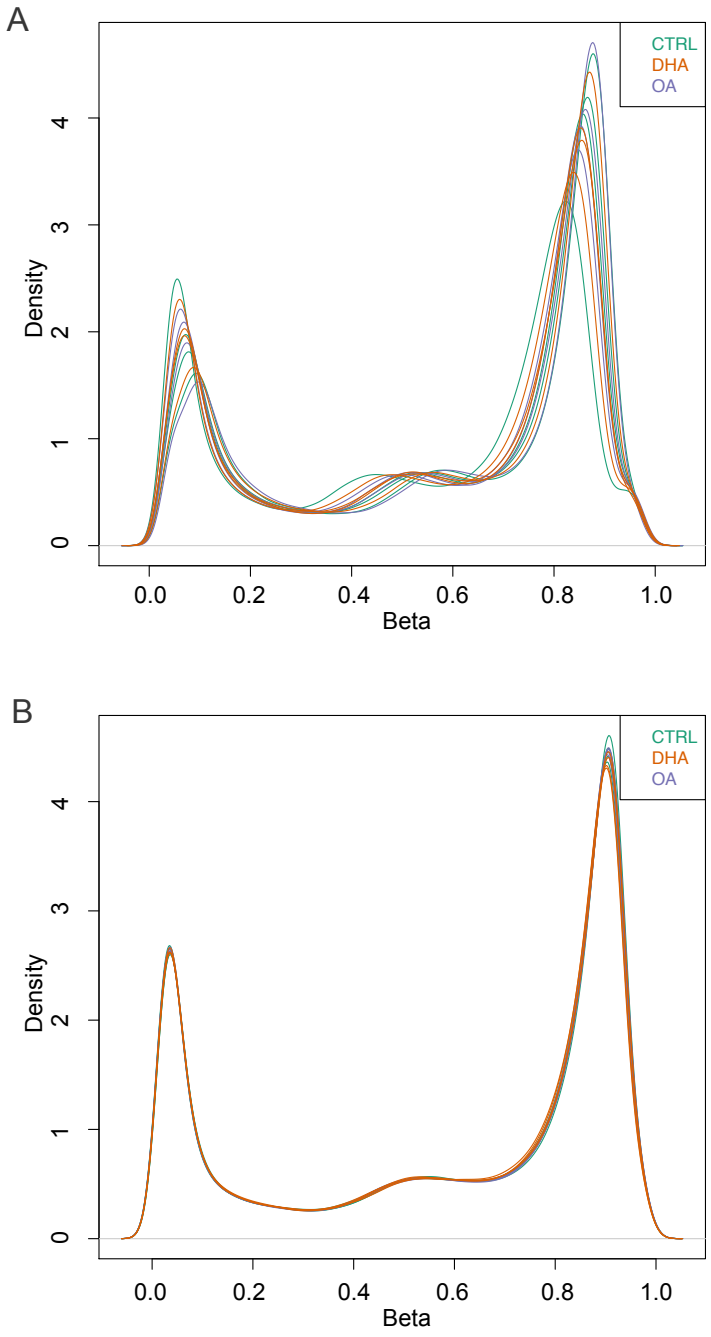

850K Array β-density distribution before (A) and after normalization (B) using Funnorm pre-processing (minfi R package).

Supplemental Figure 2.

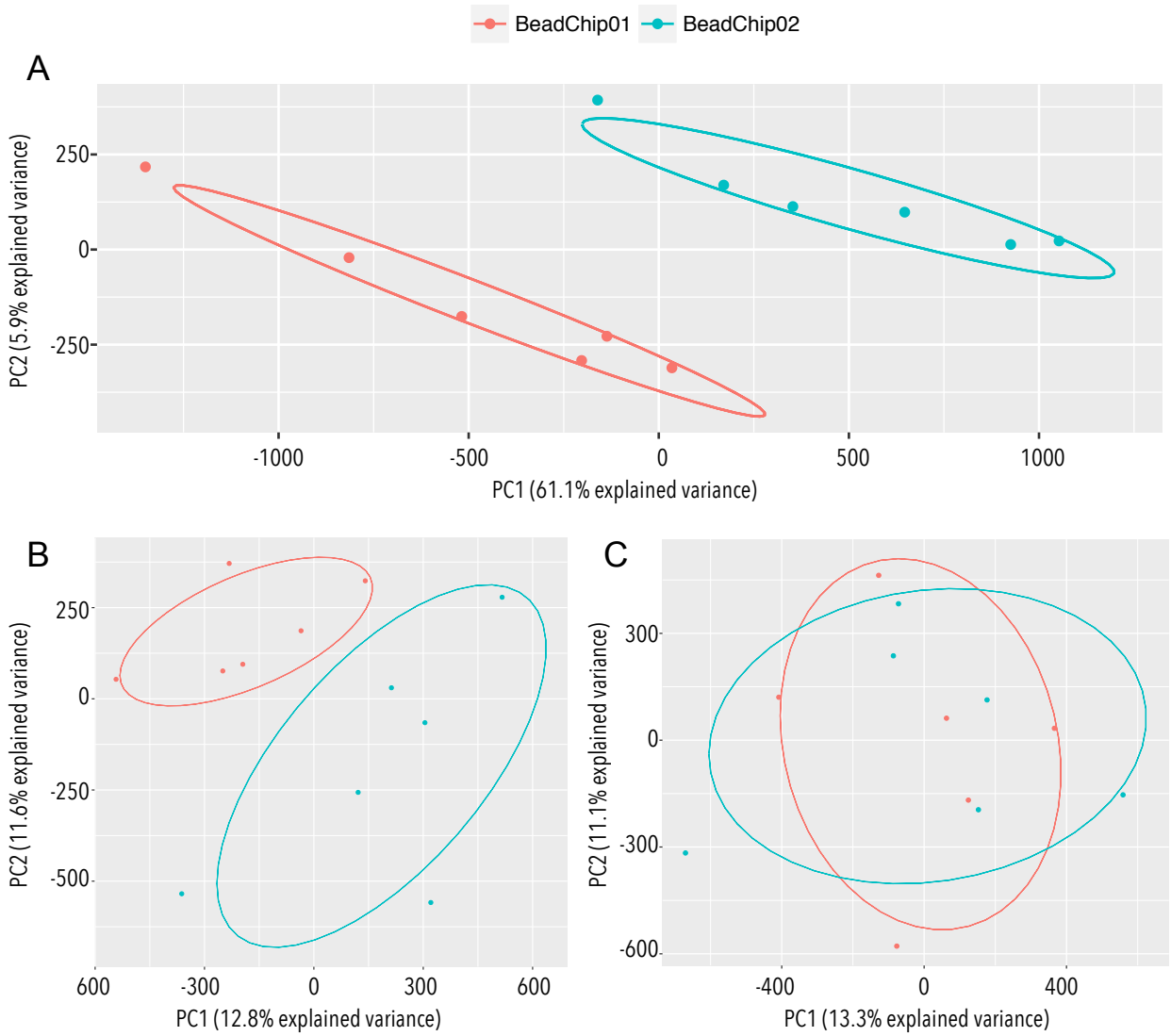

Principal component analysis (PCA) of samples showed a batch effect on the raw methylation values (preprocessRaw) (A). The batch effect was partially corrected after Funnorm pre-processing (B) and was lost after application of the Combat tool (C). Each BeadChip analysed the same number of culture replicates (n = 2 per treatment group). Thus, differences identified by PCA could not reflect differences due to treatments (CTRL, 22:6n-3 or 18:1n-9).

Supplemental Figure 3.

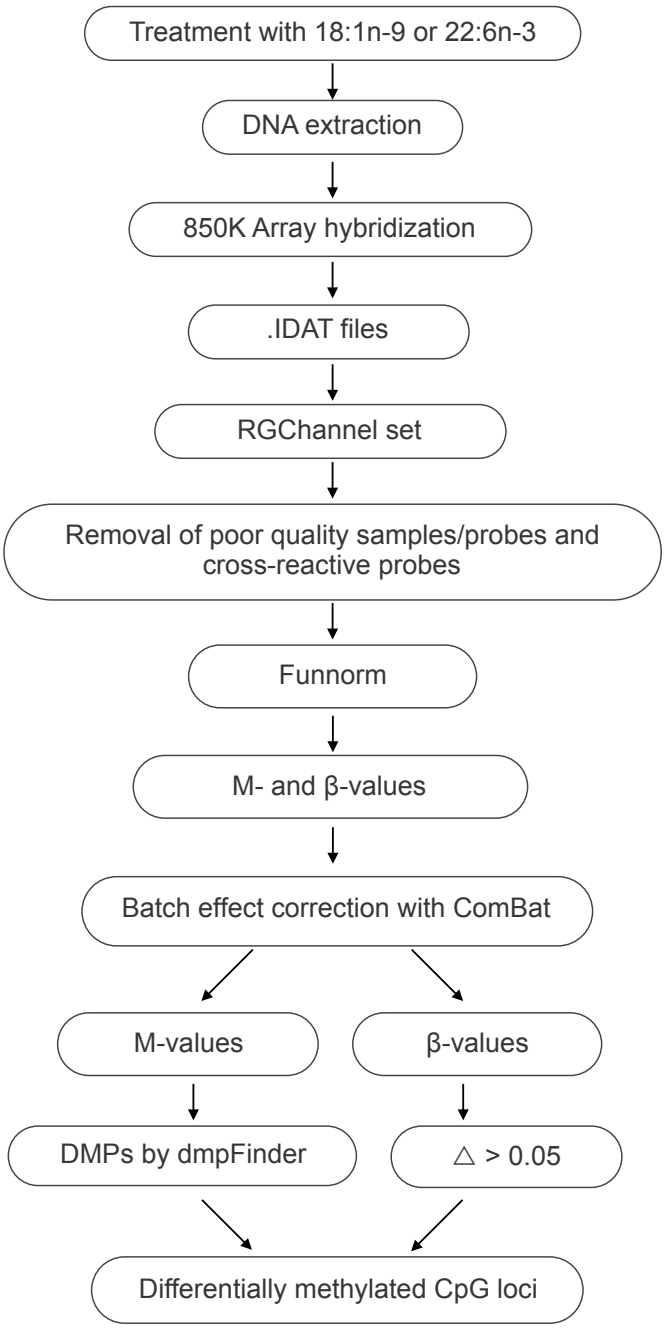

Overview of 850K analysis workflow using R package minfi. Funnorm, Functional Normalisation; DMPs, differentially methylated positions; Δ, difference from controls.

Supplemental Figure 4.

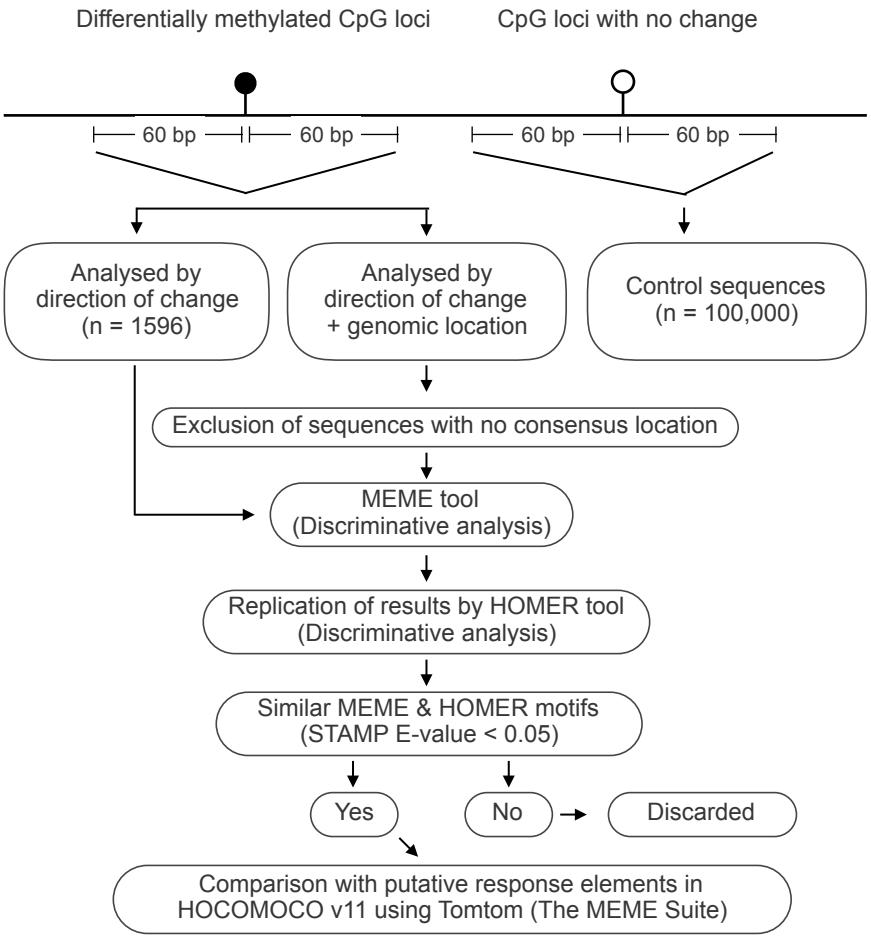

Overview of DNA motif analysis workflow. MEME, Multiple Expectation maximisation algorithm for Motif Elicitation; HOMER, Hypergeometric Optimisation of Motif EnRichment; STAMP, similarity, tree-building, and alignment of DNA motifs and profiles; HOCOMOCO, HOmo sapiens COmprehensive MOdel Collection.